Nuclear Instruments and Methods in Physics Research B 345 (2015) 42–47

Contents lists available at ScienceDirect

Nuclear Instruments and Methods in Physics Research B

journal homepage: www.elsevier.com/locate/nimb

External-RBS, PIXE and NRA analysis for ancient swords

Hellen C. Santos *, Nemitala Added, Tiago F. Silva, C.L. Rodrigues

Instituto de Fisica da Universidade de Sao Paulo, Caixa Postal 66318, 05315-970 Sao Paulo, SP, Brazil

ARTICLE INFO

Article history:
Received 13 November 2014
Received in revised form 19 December 2014
Accepted 22 December 2014
Available online 13 January 2015

Keywords:
Ion beam analysis
External PIXE and RBS setup
NRA
Cultural heritage objects
Archaeometry

ABSTRACT

Elemental composition of the steel of two ancient swords (Japanese and Damascus from a private collection) was characterized using in air IBA techniques. Our results contribute for the understanding the processes of manufacturing (hammering and quenching) and surface treatments applied in these swords. The Particle Induced X-ray Emission (PIXE) measurements along the Damascus blade allowed to identify and to trace a superficial concentration profile for the elements such Cr, Mn, Fe, Ni, Cu, Zn and As, while results for the Japanese blade showed only the presence of iron. The carbon content on the surface was also investigated using a resonant region in the Elastic Backscattering Spectrometry (EBS) measurements and the results have shown a slightly difference between the surfaces under investigation. In order to investigate the nitrogen content on surface, that could explain the hardening process, we used Nuclear Reaction Analysis (NRA) and the results shown that nitrogen content was under our detection limit for the technique (0.3% in mass). The measurements of PIXE, NRA and EBS were taken using the external beam setup installed at Lamfi – São Paulo/Brazil, the latter being successfully implemented for the first time in this facility.

1. Introduction

Undoubtedly, Japanese swords and Damascus swords have always been considered the most famous sword of the world, both from stylistic point of view and peculiar performances.

In order to understand the differences of these swords it is important to identify and quantify the influence of the iron ore and forging process. According to Bhardwaj [1], the superiority of the Indian steel could be related to the high quality of the Indian iron ores. Besides that, since it was prepared in small quantities and at a low heat, there is an incomplete reduction of iron oxides and practically absence of other oxides. On the other hand, in the native methods of manufacture, the molten steel was slowly cooled down in the crucible, which is advantageous to the material (cementation process). The Indian steel, usually referred to as wootz, was commonly made by a method resembling the modern cementation process or crucible process, where small pieces of wrought iron were packed into crucible with chopped dry wood or charcoal and leaves of specific plants e.g. *Avaram* (*Cassia auriculata*). Then the crucibles were sealed with clay and staked into a furnace which was maintained at high temperature. Afterward, the mixture formed was forged directly into a blade shape by many repeated heating and hammering operations, at low temperature.

As reported by Wadsworth, and Sherby [2], the wootz steel contains about 1.5% of carbon by weight, plus low levels of other impurities such as silicon, manganese, phosphorus and sulfur. In the forging process the control of the temperature is important to form the crystalline structures as cementite that gives the hardness to the blade. The hardening of the edge were made by heating the blade to 1000 °C, then it was air cooled down to 700 °C and quenched in brine before to reach warm temperature (~37 °C) .

In "The Craft of the Japanese Sword" [3], the author discuss minutely about how is the process to make Japanese sword. The sophisticated process requires steel with two different amount of carbon, about 0.7% which was used in the "jacket steel" – called *kawagane* – that is used in the outer surface of the blade, and low-carbon steel (below 0.5%) which was used in the core – *shingane*. The *shingane* is embedded or wrapped in the high-carbon steel along the entire length of the sword. Being more ductile than *kawagane*, this method gives to the blade a soft core that helps to protects it against cracking or breaking under stress. Since the *kawagane* requires final content of 0.7% of carbon, the smith starts the forging process with a steel of high quality containing carbon from 1.0% to 1.5% – *tamahagane*, since the forging process cause a continuous loss of carbon. The process involves several cycle of folding, hammering and heating the steel [3]. Thus, we expect that Japanese blade present less carbon and more pure steel than Damascus blade. Meanwhile, for Damascus blade, the nitrogen in the surface is expected, since in hardening the edge the blade usually was quenched in brine or animal urine, which contains a significant concentration of nitrogen [2].

* Corresponding author.
E-mail address: hellencsa@gmail.com (H.C. Santos).

http://dx.doi.org/10.1016/j.nimb.2014.12.076
0168-583X/

Although the carbon content (according to [4], for Damascus blade about 2 wt% of carbon) was cited as the main element that can give the hardness to the Damascus blades, it was verified in the same work that even in low concentration (<100 ppm) the elements Mn, Cr, Ni and Cu could play a fundamental role in the formation of crystal structures as carbides responsible for the typical Damascus patterns. However, the Japanese blade present an extraordinary cut power too, even though its purest are steel composed practically by a mixture of carbon and iron.

In this work, we propose a non invasive study in order to evaluate the differences of the Damascus and Japanese swords, using in-air PIXE and EBS techniques. In-air PIXE and EBS analyses are largely applied when a non-destructive approach is mandatory, since no sampling is required. Results of studies using PIXE and EBS [5–7] for characterization of alloys used in artwork have been reported with good results. PIXE and EBS analysis can be complementary each other, whereas PIXE is a multi-elemental analysis (able to determine and quantify elements from $Z > 13$), and EBS/RBS can be used to obtain the thickness and depth profile for elements with $Z < 13$, where the PIXE is less efficient.

2. External IBA set-up

The RBS and PIXE measurements were performed at external beam setup of the Lamfi (Laboratory of material analyses using ion beams – São Paulo University) using a Tandem accelerator of 1.7 MV. In this setup detectors and instrumentation are mounted in 7 geometrically collimated ports distributed along a conical surface at an angle of 135° in relation of the beam direction. The collimation system allows simultaneous measurements of the same irradiation area for the diverse techniques. This setup was originally planned to avoid signals from other sources, due to the restriction imposed to the detector solid angle, being important, for example, in the mitigation of the argon signal from the air in the PIXE measurements [8]. For PIXE analysis, two X-rays detectors Si(Li) with resolution of 160 eV (FWHM@MnKα) are mounted in two symmetrical positions, and the filters used in each one defined the sensitive interval for elemental identification.

Recently the external setup was improved with a surface barrier detector installed in one of the ports, enabling the detection of scattered particles (RBS/EBS) at 135°. In order to improve RBS resolution a He gas supply was provided to reduce energy losses and straggling in the external environment. A schematic of the RBS setup for the external beam is presented in Fig. 1.

Two windows are important in the RBS analysis: a 6 μm thick aluminum foil mounted in the end of the beam line, and a 12 μm thick Mylar mounted in the port of the RBS detector. In principle, the setup was optimized for protons.

3. Experimental procedure

The regions analyzed in the Damascus (6) and Japanese (4) blades are presented in the Fig. 2. These regions were polished with sandpaper to remove the oxidation layer and then cleaned with alcohol. In order to establish a difference between the cut edge and the body of the blades, we performed PIXE and EBS measurements of two spots for each region (regions 1–6 for Damascus blade, and 1–4 for Japanese blade), one close to the cut edge and the other about 4–5 mm far from the cut edge.

3.1. PIXE measurements

The PIXE measurements were used to identify the elemental composition along both swords, verifying eventual contributions of manufacturing and treatment processes in their relative concentrations. In our measurements we used a 2.6 MeV internal proton beam, corresponding to 2.365 MeV on the target, accordingly SRIM [9] simulation (with 14 keV energy straggling). The dose normalization was made using the gamma rays from the aluminum window, due the reaction $^{27}Al\ (p,p)^{27}Al^{*}$ produced at the vacuum window and collected by a NaI(Tl) detector.

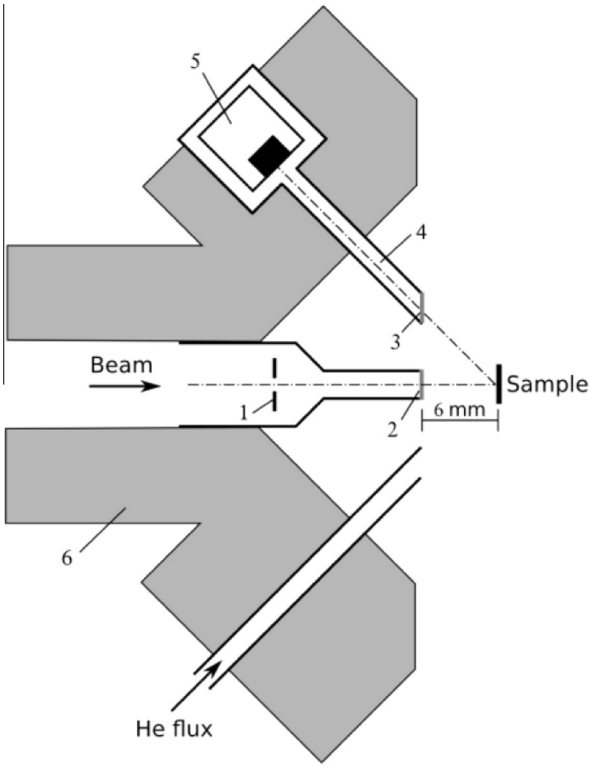

Fig. 1. Schematic of the in-air RBS setup. (1) 1 mm diameter beam collimator; (2) 6 μm thick aluminum vacuum window; (3) 12 μm thick Mylar vacuum window; (4) rough vacuum environment; (5) surface barrier detector; (6) mechanical support structure [8].

Typical PIXE energy spectra are presented in Fig. 3 for the two swords under investigation and for the standard CRM 298.

3.2. EBS measurements

The EBS analysis can contribute to differentiate in more detail the steel of the ancient swords under investigation given information about carbon concentration that is out of the limit detection of PIXE technique, typically low Z elements ($Z < 10$). To measure small quantities of a light element in a matrix composed of heavy elements, is important to use resonant reactions. It is also very important verify the non-Rutherford cross section of neighbor elements, avoiding resonances near from the resonance of interest. As some of the surface treatments generate carbon compounds, the carbon content in the surface was investigated using the reaction $^{12}C(p,p_0)^{12}C$. This particular reaction presents a high intensity resonance (@1.735 MeV), as we can see in the Fig. 4.

An important step in this analysis is adjust the internal energy of the proton beam to ensuring that the resonance occurs in the surface of the target. To obtain this energy it must to be taken into account the stopping power of the protons in the aluminum window and in the artificial atmosphere (air + helium) in the path of the beam (6 mm – the distance between the vacuum window and the sample surface). The energy tune was made using a sample of Ultra Dense Amorphous Carbon (UDAC) and the optimum value for the internal beam energy was 2.0 MeV. Details of this procedure

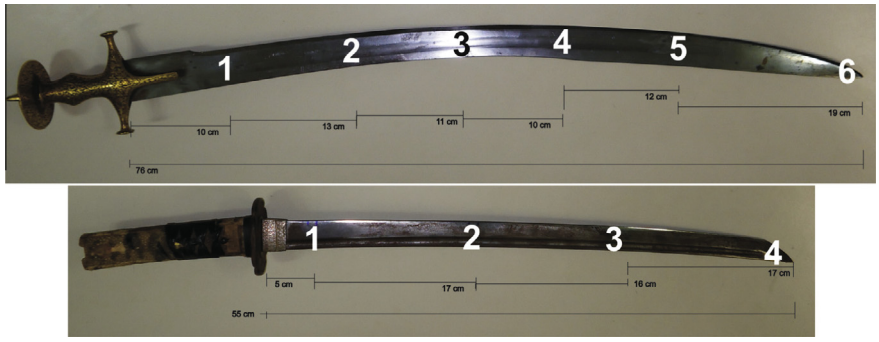

Fig. 2. Picture of the Damascus blade (top) and Japanese blade, indicating the dimensions and areas irradiated.

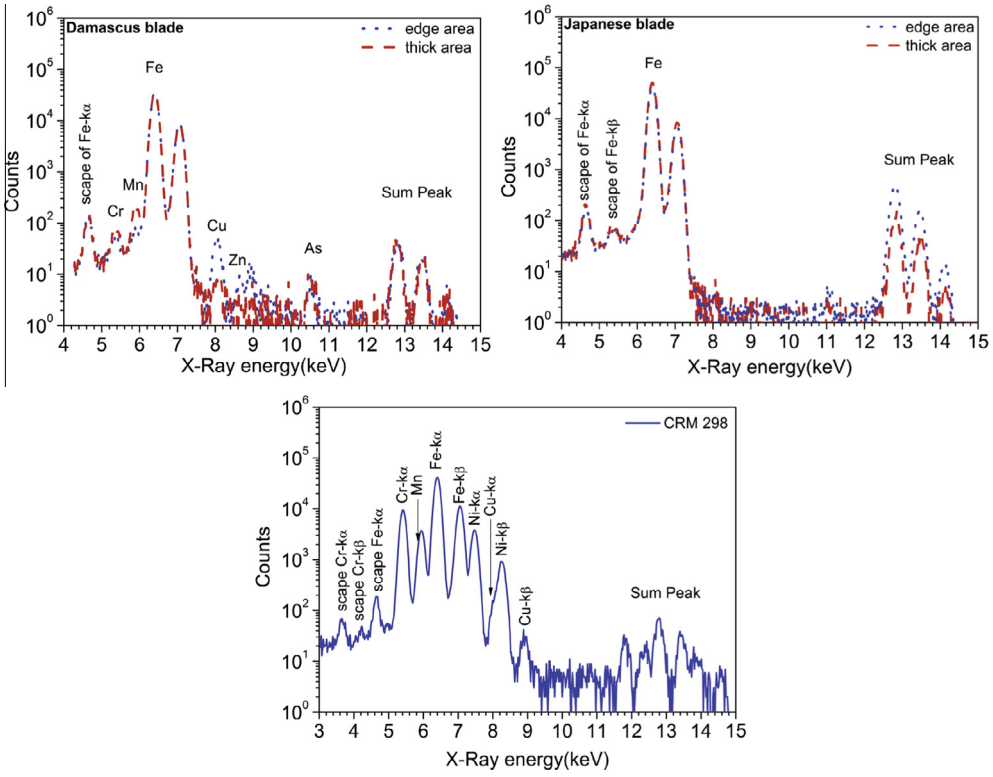

Fig. 3. Typical in-air PIXE spectra of Damascus and Japanese blades and the standard CRM 298. In each spectrum are shown the edge and thick spots measured. The identification of the picks were performed using the software QXAS [10].

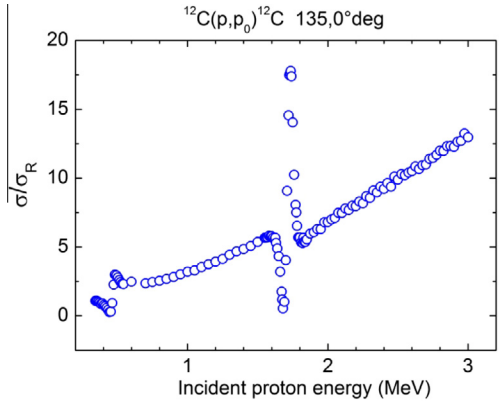

Fig. 4. Elastic scattering cross section for protons with energy range 0.34–3.0 MeV for the reaction $^{12}C(p,p_0)^{12}C$ at 135° [11].

are described in Silva et al. [8]. This value of energy was used as default for all EBS measurements mentioned in this work. Several measurements were performed on both swords and the typical RBS spectra of Damascus and Japanese blades are presented in the Fig. 5.

3.3. NRA measurements

NRA technique can be used to investigate light elements in a matrix of heavy elements, but in this case we use nuclear reaction that involves γ-ray production. The nitrogen content in the surface was checked using the reaction $^{15}N(p, \alpha\gamma)^{12}C$, since in its γ-ray production cross section there is a high intensity resonance that occurs at the 1.64 MeV proton beam. These measurements were performed in different condition at Lamfi, with an internal proton beam of 1.8 MeV that produces a 1.6 MeV on the surface of the target. Several measurements were performed on both swords and

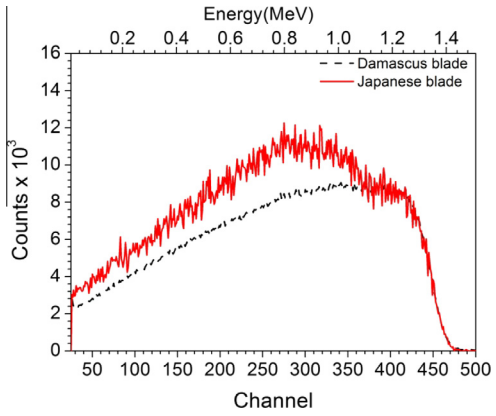

Fig. 5. Typical RBS spectra of spots in Damascus blade and Japanese blade.

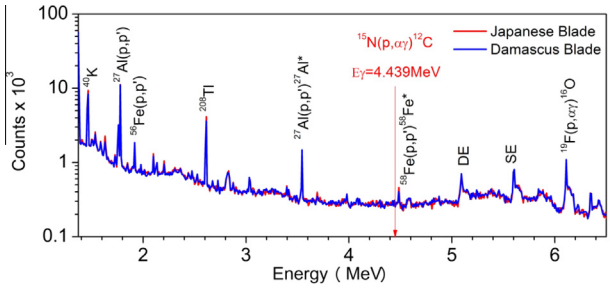

Fig. 6. Typical NRA energy spectra of spots in Damascus and Japanese blades. In plot are identified some peaks resulting of the 1.8 MeV proton beam on the Al window and the blades (^{58}Fe(p,p′)^{58}Fe*) as well as the background peaks ^{40}K (Eγ = 1.46 MeV) and ^{208}Tl(2.614 MeV).

pure iron (used to background subtraction). The typical NRA spectra of Damascus and Japanese blades are presented in the Fig. 6.

4. Results and discussions

4.1. Elemental composition of the matrix

The PIXE data was analyzed using the software QXAS [10] that provide the areas under the identified peaks as well as the background counts. Relative area of the elements resulting from PIXE analyses are shown in the plots of Fig. 7, these relative areas were evaluated by the ratio of each element and the sum of all identified elements, which Fe corresponds of more than 95%. In these plots we can see the distribution of the identified elements along the Damascus blade for the two measured spots in each region for the elements Cr, Mn, Fe, Ni, Cu, Zn, and As. The PIXE analysis of Japanese blade indicated just the presence of Fe with no trace elements in the matrix.

The results indicate distinctly differences in the steel used for manufacturing these two blades. In fact, the composition of the steel reflects directly the origin of iron ore but the manufacturing process is also important, as shown by [12]. In their work, using destructive measurements to characterize several Indian ancient swords, C, P, S, Si, Ti, V, Cr, Mn, Ni and Cu were identified as part of steel matrix. In our work, in a non-destructive way, we identified most of these elements. Moreover, in order to quantify the identified elements and allow the comparison with other sources, we performed PIXE measurements in a steel standard sample for evaluating the self-absorption. For this purpose, we also measured a CRM 298 (EURONORM-CRM duplex stainless steel) to evaluate the Mn, Cr, Ni Cu contents.

It was verified that the relative area for the Cr, Mn and As, are systematically higher for the cut edge region. For Ni, Cu and Zn the higher relative areas were found in the thick area. The relative concentrations tend to decrease towards the hilt to the tip of the blade (except for Mn), suggesting that the forge process, heating and hammering the steel from a unique ingot, as expected for Damascene blades, can cause a redistribution of the elements along blade.

For the elements Cr, Mn, Ni and Cu we evaluated the absolute concentration, using the standard CRM 298, and results are given as percentage in mass in the Table 1. In this calculation we assumed that the sum of the elements Fe, Mn, Ni and Cu was 100% of the steel, where the contribution of Fe in this sum is of order of 95%. The sum of the same elements in the standard is of order of 96%, wherein the Fe contribution is 63%. The sample was considered homogeneous in a range of approximately 24 μm that corresponds to the analyzed depth, which in this case is completely defined by the proton range in a sample with an iron matrix. Assuming that, in this depth the concentration is uniform, and the swords and standard are compatible, thus the self-absorption was taken in account by comparing the sample with a standard in order to get elemental concentration. Depending on the content of these elements in the steel, they can improve mechanical properties like hardness, resistance to corrosion or heat resistance as we can see in the Table 1.

The L_D (detection limit of Curie [14]) for PIXE procedure was obtained using the counts of background of the standard spectrum. Considering the L_D for each element in the Table 1, we can suggest that Mn can contribute to the hardness in both analyzed areas, although the higher values presented were in the thick area and not in the cut edge as we would expected due to their cut characteristics. The content of Cu may contribute to the corrosion resistance also to the both analyzed areas. The Ni is out of the detection of quantification.

4.2. Carbon content evaluation

EBS analysis was used specifically to investigate the presence of carbon on the surface of the blades. In order to improve the sensitivity in the carbon identification we decided to subtract the iron contribution on each EBS spectrum. For this purpose, we irradiated a sample of pure iron in the same experimental conditions used in the irradiation of the swords. In the Fig. 9 we compare normalized EBS spectra of Japanese and Damascene blades after subtraction of the pure iron spectrum that is shown in Fig. 8.

It can be noted a clear difference in the EBS spectra of the swords. To show the presence of carbon contribution in these two spectra we add to the same plot the EBS spectrum obtained irradiating a UDAC sample in the same experimental conditions, and a simulated curve for oxygen (using SIMNRA). A qualitative analysis indicates that the carbon content in the surface of Japanese seems higher than Damascus blade, since the resonance of the reaction ^{12}C(p,p$_0$)^{12}C with a 2.0 MeV proton beam could be used to adjust in an appropriate way the EBS spectrum just to Japanese sword, as shown in Fig. 9.

It is also possible to see a negative contribution on both spectrum of Japanese and Damascus blade for higher channel values. This negative contribution is due to the difference of oxygen on the surface for the swords when compared with the pure iron, suggesting that the cleaning process was not complete and that an oxidized layer still remain.

4.3. Nitrogen content evaluation

One important step in the determination of the content of nitrogen in the blades surfaces is to evaluate the counts of nitrogen

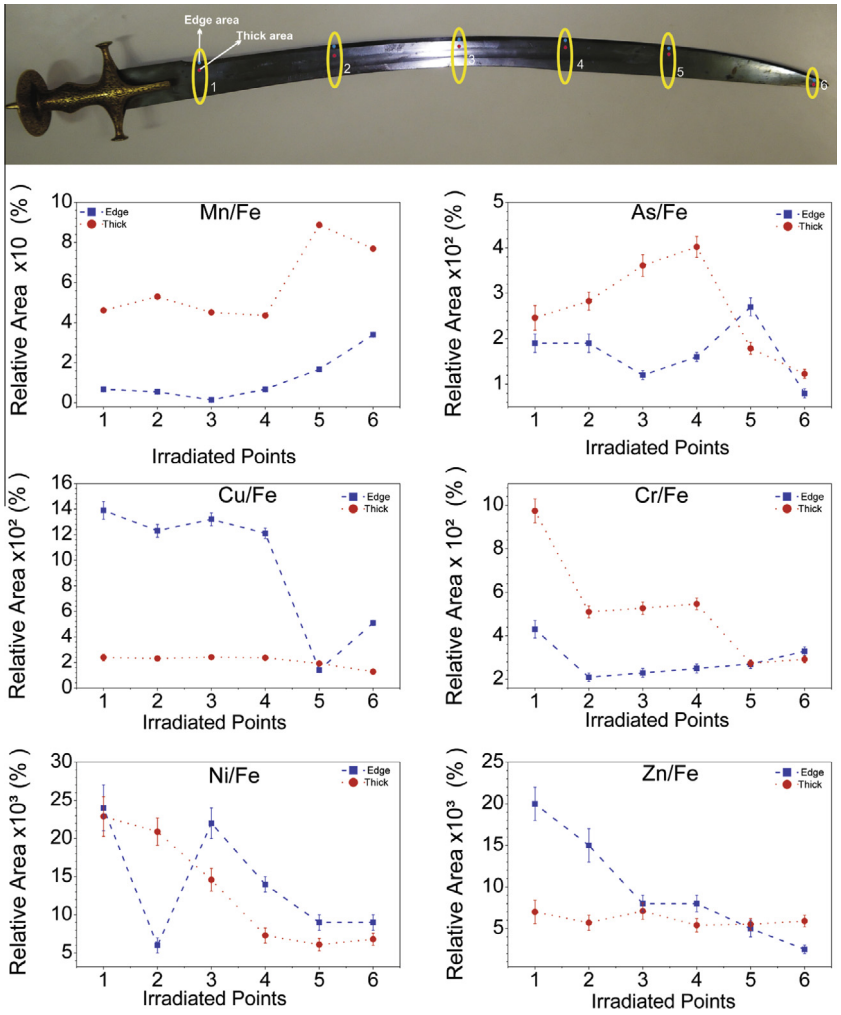

Fig. 7. Behavior of identified elements along the Damascus blade. The irradiated spots are identified on the top (Damascus blade picture).

Table 1
Contents of some elements measured in the two analyzed areas of the Damascus blade.

Element	Cut edge content (%)	Thick area content (%)	Recommended[a] content (%)	Property performed on steel	L_D[b] content (%)
Cr	0.037–0.076	0.049–0.17	11.0	Corrosion resistance	0.036
Mn	0.008–0.2	0.26–0.53	0.23–0.9	Hardness, desulfurize	0.015
Cu	0.011–0.11	0.01–0.023	min. 0.01	Corrosion resistance	0.015

[a] Recommended values [13].
[b] Detection Limit of Curie converted in concentration [14].

from the air in the energy spectrum. The procedure applied to subtract this contribution was to measure a pure iron sample, since the sample is almost composed by iron as we saw in PIXE results. Finally, to quantify the nitrogen content we also measured a standard steel sample (CRM 298) that contains a nominal value of 0.263(4)% in mass of nitrogen.

After subtracting the background of the CRM 298 gamma energy spectra, the nitrogen content calculated was lower than 0.3% with a high uncertainty, indicating the limitation of our setup to measure this reaction. Efforts to reduce this uncertainty by increasing the time of acquisition were no efficient. Thus we conclude that the detection limit of our setup is around 0.263%. In the plot of Fig. 10 the comparison of CRM 298 and pure iron spectrum are shown, the interest area is shown in the detail. It is evident that the whole spectra match with pure iron spectra except for the region from 3.5 MeV to 5.0 MeV, where the gamma from the decay of carbon from $^{15}N(p, \alpha\gamma)^{12}C$ reaction should be, as

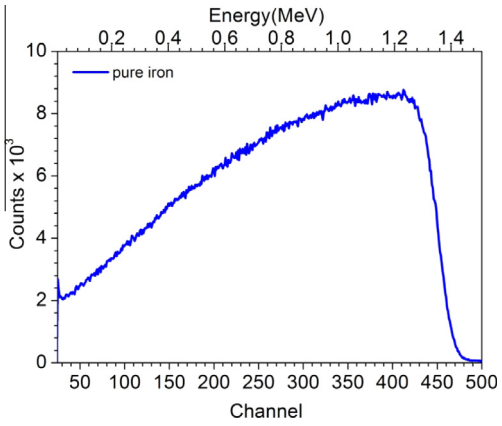

Fig. 8. Typical RBS spectrum of 2.0 MeV protons scattered of pure iron.

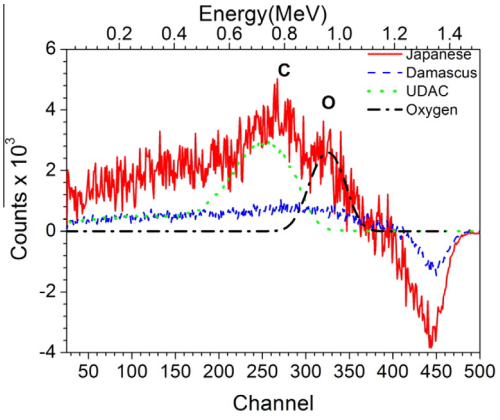

Fig. 9. EBS energy spectra of 2.0 MeV protons scattered from Japanese blade, Damascus blade and UDAC. The spectra were normalized by pure iron RBS spectrum them it was subtracted of the Japanese and Damascus spectra. The UDAC spectrum was also plotted in order to show the carbon resonance of the reaction $^{12}C(p,p_0)^{12}C$ with a 2.0 MeV proton beam, and the oxygen data is a SIMRA simulation in same conditions of the experiment.

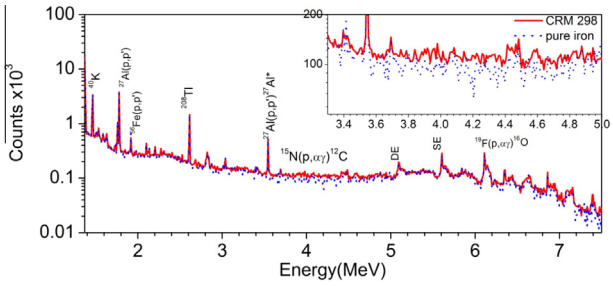

Fig. 10. Gamma energy spectra CRM 298 and pure iron samples. In the detail is shown the interest area ranging from 3.5 to 5.0 MeV. SE and DE are first and second escape, respectively, due to the pair production in the detector from the reaction $^{19}F(p,\alpha\gamma)^{16}O$.

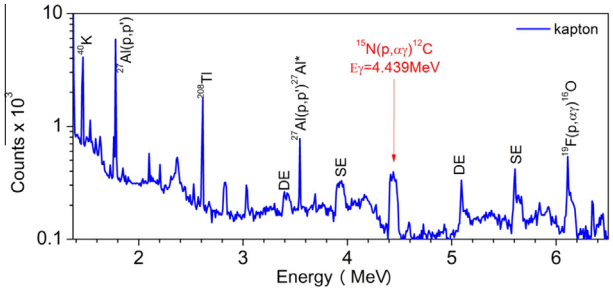

Fig. 11. Gamma energy spectra of kapton, the typical structure of γ-ray from the first excited state of ^{12}C appear in 4.4 MeV with its escapes (DE and SE).

shown in Fig. 11 for measure performed in a 12 μm thick kapton foil (chemical composition of kapton: $H_{10}C_{22}N_2$ – 5.13% in atoms of nitrogen).

In Fig. 12 are shown the gamma energy spectrum for the Japanese blade, Damascus blade and the pure iron, with no evidence of the γ-ray from the decay of ^{12}C, in order to this pick the kapton spectra also was plotted in the interest range (from 3.5 to 5.0 MeV). As one possibility typical nitriding process to hardening surfaces can introduce nitrogen in 5–15 μm range. To explain the lack of nitrogen on Damascus blade is the polishing procedure to remove the oxidized layer. Anyway, if there is any nitrogen content in the surface, certainly this amount is less than 0.3% in mass.

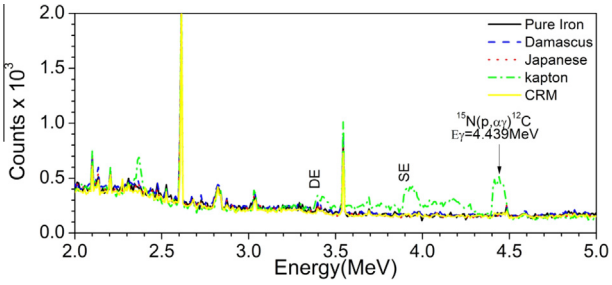

Fig. 12. Comparison of gamma energy spectra for Japanese blade, Damascus blade and pure iron, kapton and CRM 298 in the interest area ranging.

5. Conclusion

It was shown in this work the first results for the new external RBS setup installed at Lamfi, that can be largely applied for cultural heritage when the non-destructive analysis is mandatory, whence this new setup allows measurements of large object whose dimensions, brittleness and cultural values prevents them from being placed in a vacuum environment. Our results for carbon analysis suggest that carbon is the only element that can be related to the hardness in the Japanese sword. In the other hand, carbon contribution for damascene sword, contrary to expectations, is not compatible with other results in the literature. Finally, PIXE results have shown different elemental composition for the both swords, similar to other published values. One important point in our study is that all analysis can be made simultaneously, thus complementing the investigation to a better understanding of the artwork under study.

Acknowledgments

Thanks to Diogo Emiliano, who kindly lent us their swords. This work was supported by CAPES (Coordenação de Aperfeiçoamento de Pessoal de Nível Superior) and CNPQ (Conselho Nacional de Desenvolvimento Científico e Tecnológico – Brasil).

References

[1] H.C. Bhardwaj, Development of iron and steel technology in India during 18th and 19th centuries, Indian J. Hist. Sci. 17 (2) (1982) 223–233.
[2] J. Wadsworth, O.D. Sherby, On the Bulat – Damascus steel revisited, Prog. Mater. Sci. 25 (1) (1980) 35–68.
[3] L.K.Y. Yoshihara, H.K.Y. Yoshihara, The Craft of the Japanese Sword, Kodasha International Ltd., USA, 1987.
[4] J.D. Verhoeven, A.H. Pendray, W.E. Dauksch, The key role of impurities in ancient Damascus steel blades, JOM (September 1998).
[5] M. Noun, M. Roumie, T. Calligaro, B. Nsouli, R. Brunetto, D. Baklouti, L. d'Hendecourt, S. Della-Negra, On the characterization of the "Paris" meteorite using PIXE, RBS and micro-PIXE, Nucl. Instr. Meth. B 306 (2013) 261–264.
[6] M.F. Guerra, T. Calligaro, Gold cultural heritage objects: a review of studies of provenance and manufacturing technologies, Meas. Sci. Technol. 14 (2003) 1527.
[7] M.A. Rizzutto, M.H. Tabacniks, N. Added, M.D.L. Barbosa, J.F. Curado, W.A. Santos Jr., S.C. Lima, H.G. Melo, A.C. Neiva, The external beam facility used to characterize corrosion products in metallic statuettes, Nucl. Instr. Meth. B 240 (1–2) (2005) 549–553.
[8] T.F. Silva, N. Added, M.V. Moro, G.F. Trindade, H.C. Santos, C.L. Rodrigues, M.A. Rizzutto, M.H. Tabacniks, In-air RBS measurements at the LAMFI external beam setup, AIP Conf. Proc. 1625 (2014) 120.
[9] J.F. Ziegler, SRIM-2003, in: Proceedings of the Sixteenth International Conference on Beam Analysis, vols. 219–220, June 2004, pp. 1027–1036.
[10] Quantitative X-ray analysis system (QXAS) software package, IAEA, Vienna, Version 1994.
[11] S. Mazzoni et al., Nucl. Instr. Meth. B 136–138 (1998) 86.
[12] D.T. Peterson, H.H. Baker, J.D. Verhoeven, Damascus steel: characterization of one Damascus steel sword, Mater. Charact. 24 (1990) 355–374.
[13] V. Chiaverini, Aços e Ferros Fundidos, seventh ed., Associação Brasileira de Metalurgia e Materiais – ABM, 1996.
[14] L.A. Currie, Limits for qualitative detection and quantitative determination. Application to radiochemistry, Anal. Chem. 40 (3) (1968) 586–593.